

# High Performance System-on-Package Integrated Yagi-Uda Antennas for W-band Applications and mm-Wave Ultra-Wideband Data Links

B. Pan, G. DeJean, J. Papapolymerou, M. M Tentzeris, Y. Yoon and M. G. Allen

Georgia Electronic Design Center, School of Electrical and Computer Engineering  
Georgia Institute of Technology, Atlanta GA 30332-0269 USA  
Tel:(404) 385-6402, Email: panbo@ece.gatech.edu

## Abstract

This paper reports two System-on-Package (SoP) integration schemes for utilizing the Yagi-Uda antenna in the RF/Microwave/millimeter wave applications. A substrate independent W-band vertical Yagi-Uda was fabricated and characterized. It shows a forward gain of 5.3 dBi and a front-to-back ratio of 6 dB and has proofed the feasibility of using the surface micromachining technology into SoP integration. A compact mm-wave printed Yagi array is also reported for the first time with a 12.0 dBi gain achieved.

## I. INTRODUCTION

Emerging wireless communication and sensor applications in the RF/Microwave/millimeter wave regimes require low loss and high performance antennas. A good antenna design for these new circumstances is not just simply scaling classical antenna to different frequencies, but also to meet different operating requirements. In many applications, an end-fire radiation pattern is needed to have the electromagnetic wave propagate along the supporting substrate. To generate this pattern, an exponentially or linearly tapered slot antenna (TSA) can be used. However, its drawbacks such as relatively large overall size and relatively high cross-polarization level have prevented it being widely used when these inherent drawbacks can not be accepted. Log periodical antenna has also been extensively studied in the past several decades for endfire applications. It provides an ultra wide bandwidth and almost constant end-fire radiation pattern at the same time. But the requirement for the long boom length has limited its application. Another candidate is the Yagi-Uda antenna. It has been used for almost eight decades since Uda and Yagi first investigated it in 1920's. It consists of a driven element, a reflector and several directors. Only the driven element is directly fed by source while the others are parasitically coupled. Since only a few elements for a Yagi-Uda array needs to be fed directly, the introduced simplicity has made it find many applications including outdoor TV signal receiving.

In SoP integration, many function (digital, RF, optical, etc) modules need to be implemented on a single type of wafer and package [1]. However, traditional Yagi-Uda antennas used for HF and UHF application are usually built by several metal rods and not well suited for integration. A printed version was first proposed by J. Huang [2] in 1989 and much progress has

been done in recent years. Despite of this advances, few integration efforts of Yagi-Uda antenna have been put onto W-band and WLAN applications.

This paper reports two System-on-Package (SoP) integration schemes for utilizing the Yagi-Uda antenna in the RF/Microwave/millimeter wave applications. The first one is for W-band applications and features the utilization of the advanced surface micromachining technologies. The second one is designed for mm-wave ultra-wideband data/video links, which is compatible with printed circuits process.

The W-band Yagi-Uda consists of several vertical metal posts standing on top of wafer. Instead of using dipole array, this vertical antenna uses monopole array with the help of the ground plane on top of wafer. The ground also helps isolate unfavorable substrate effects. The driven monopole is fed by a novel coplanar waveguide transition. Several prototypes have been built to investigate the director's impact to directivity. Two major merits of this vertical Yagi-Uda are wideband and low loss due to the elimination of the substrate effects. The high-aspect-ratio surface micromachining technology is used to build the metal-coated-epoxy core posts. The process is low-temperature and fully CMOS compatible, allowing easy integration with other components to meet integration needs.

In this paper, we will also present an mm-wave printed microstrip Yagi design for point-to-point ultra-wideband transmission (e.g. wireless video), that consists of two microstrip Yagi arrays that are fed simultaneously to create a "double-printed" Yagi antenna array. The operational frequency is 32.5 GHz. The conventional approach of using two microstrip Yagi arrays aligned parallel to each other caused significant backside radiation ( $\varphi \approx 180^\circ$ ). When the Yagi arrays are excited simultaneously, constructive field interference occurs and the maximum radiation lies in the positive x direction ( $\varphi \approx 0^\circ$ ) with respect to the azimuth plane. The feeding structure for this design is printed on the same surface with the elements in order to simplify the structure and maintain inexpensive manufacturing costs. The relative impedance bandwidth for this design is around 8% which is due to the combination of two resonances at frequencies above and below the operational frequency. The co-polarized component of the E-plane elevation pattern exhibits a maximum radiation at approximately  $35^\circ$  with a beamwidth of

40° between  $\theta = 20^\circ$  and  $\theta = 60^\circ$  and a directivity close to 12 dBi can be achieved.

## II. W-BAND VERTICAL MONOPOLE YAGI UDA ANTENNA

W-band ranges from 75GHz to 110GHz. The corresponding dimension for antennas working at W-band is on millimeter scale, thus it is possible to implement a lot of classical 3-D antennas by using advanced surface micromachining technology. Negative tone photoresist SU-8 is suitable for defining high aspect ratio micromachined structures and widely used. Here, we utilized this feature to build vertical wire antenna on top of wafer.

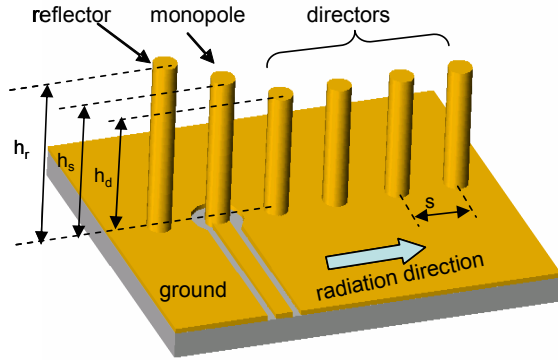


Fig. 1 The structure of W-band vertical Yagi-Uda antenna

The structure we built is shown in Fig 1. Unlike the classical wire Yagi-Uda used in UHF applications, monopoles instead of dipoles are used due to the existence of ground plane on top of wafer. The other function of the ground plane is, more importantly, isolate all kinds of substrate effects, which is the major feature we claim for this structure. Epoxy-core metal-coated posts are fabricated using surface micromachining process. The different heights of the reflector, the driven monopole and the directors are realized by multiple polymer coatings and patterning.

The variables to be optimized include reflector spacing, director spacing, number of directors, reflector height, driven monopole height and director height. The objectives include impedance bandwidth, forward gain, and front-to-back ratio. Lots of researches have been done on the optimization of the Yagi-Uda, but since here our objective is to demonstrate the substrate-independent integration approach, we used the standard design curve by P.P. Viezbicke [3]. The 3-element, 5-element and 7-element array were designed. The spacing of  $0.20 \lambda$  is chosen. The initial length of the reflector, the driven monopole and the directors are chosen based on the design table in [3]. The diameter of the monopole is set to be  $100 \mu\text{m}$  and thus the diameter to wavelength ratio is approximately 0.03 at the central point of the W-band. Corrections on the optimized lengths of the elements are made to including the effect of this specific ratio [3].

Simulation and optimization of the final lengths of the elements were done by MoM based codes NEC because NEC

can provide relative accurate results much faster than other full-wave EM simulators. The FEM-based 3-D simulator Ansoft-HFSS is used to verify the design data at the final stage. Optimized director height is not the same as the number of directors used changes from 3 to 7. However, in order to put all of the arrays on a single wafer and simplify the fabrication process, the unified height for the directors is used. Since we only want to demonstrate this integration method, we compromised between the performance and the simplicity. Therefore, the final dimensions chosen for the fabrication are  $760 \mu\text{m}$  for the reflector,  $740 \mu\text{m}$  for the driven monopole and  $630 \mu\text{m}$  for the directors.

Figure 2 shows the simulated return loss for the 5 element Yagi-Uda design. The resonance is at 97.6 GHz and the forward gain at this frequency is 9.7 dBi and the front-to-back ratio is 8.8 dB.

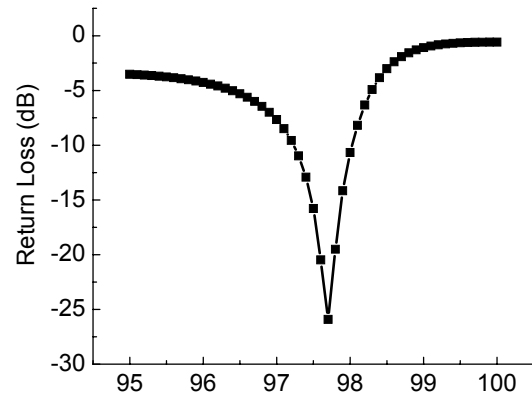


Fig. 2 Simulated return loss for 5 elements Yagi-Uda array

Fig. 3 and 4 show the simulated 2-D radiation pattern on the horizontal and vertical plane for the 7-element array respectively. With the increased directors, both the forward gain and the front-to-back ratio got improved. Numerically, for 7 elements at 94 GHz, gain is 11.9 dB, and front-back ratio is 14.5 dB. Forward gain vs. frequency is plotted in Fig. 5. The input impedance at 94 GHz is  $28.0+42.3 \text{ Ohm}$  and matching is not optimized for this design.

The fabrication procedure is described in [4][5] and is not repeated here. The measured return loss for 5-element array is plotted in Fig. 6.

The actual radiation pattern is probed by a special W-band on-wafer pattern measurement system, where the Yagi-Uda antenna is fixed and the receiving waveguide can be rotated around the antenna-under-testing. The measured forward gain for the 5-element Yagi-antenna is 5.3 dB with a 6 dB front-to-back ratio.

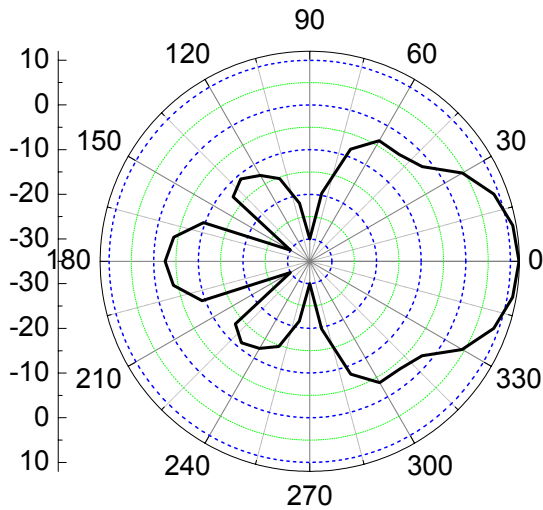


Fig. 3 Simulated 7 element Yagi radiation pattern on the horizontal plane

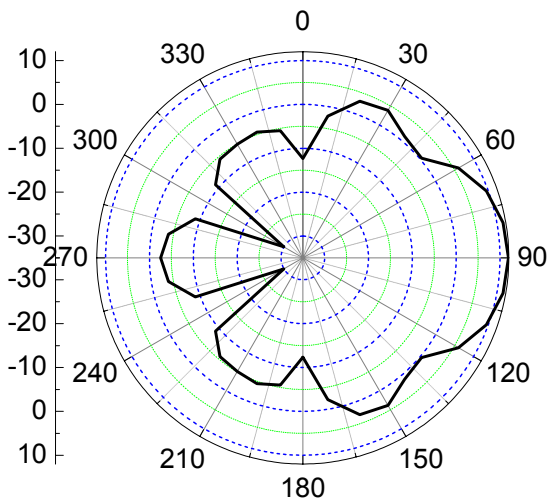


Fig. 4 Simulated 7 element Yagi radiation pattern on the vertical plane

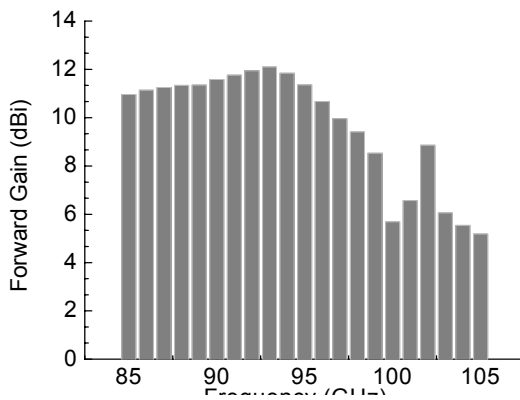


Fig. 5 Simulated forward gain vs. Frequency for 7 element array

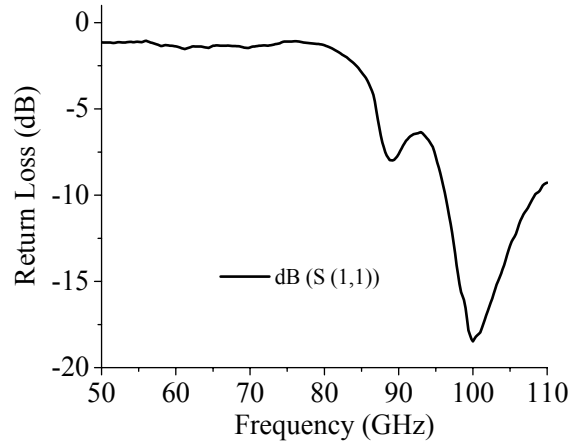


Fig. 6 Measured return loss for 5-element array

The measured data shows a fairly good directivity and has proved the effectiveness of this integration approach. The disagreement between simulation and measurement is due to the nature of prototype implementation. The process is not fully optimized to achieve designed physical dimensions. The major error comes from the coating of SU-8. The thickness of the first coating has exceeded the maximum thickness optimized by the supplier and mainly based on experience. The performance of the Yagi-Uda antenna is sensitive to the heights of the driven element. But this can be easily overcome in an industry manufacturing process where all of the fabrication conditions are optimized for a specific process.

In summary, the advantages for this integration approach include:

1. Low-temperature and totally SOP-integration compatible
2. Substrate-independent and thus can be implemented onto any substrate
3. Substrate loss and dispersion are completely isolated.

### III. MM-WAVE PRINTED MICROSTRIP YAGI ARRAY

To meet the increased interest for ultra-broadband mm-wave applications (wireless video transfer at 60 GHz at data rates in excess of 5 Gb/s for ranges up to 10m, mm-wave ad-hoc sensor networks, point-to-multipoint wideband links) that require sectorized radiation patterns (beamwidths 40-60 degrees) and high gain (above 10 dBi) in order to create quasi-omnidirectional radiation pattern and alleviate propagation loss effects, a novel printed microstrip Yagi array antenna is proposed as an effective solution for these applications. The proposed antenna structure is shown in Fig. 7. It consists of two microstrip Yagi arrays that are fed simultaneously to create a “double-printed” Yagi antenna array. The conventional approach of using two microstrip Yagi arrays aligned parallel to each other caused significant radiation in a direction 180° from the main beam in the azimuth plane [7]. In this approach, the director 1 elements are offset from the parallel configuration and the two

individual arrays are diagonally aligned to limit this radiation. As a result, the two individual microstrip Yagi arrays converge to a common director 2 element that is utilized by both arrays. One array emits maximum radiation at  $\varphi \approx 30^\circ$ , while the other array emits maximum radiation at  $\varphi \approx -30^\circ$ . When these arrays are excited simultaneously, constructive field interference occurs and the maximum radiation lies in the positive x direction ( $\varphi \approx 0^\circ$ ) with respect to the azimuth plane. All of the patch elements are square. The substrate used in the design is a 200  $\mu\text{m}$  thick sheet of RT/duroid 5880 which has a dielectric constant of 2.2 and a loss tangent of 0.0009 at 10 GHz. The operational frequency is 32.5 GHz. This frequency was chosen for proof of concept and can be easily extended to the 60 GHz range. The dimensions of the patch elements are as follows: reflectors are 4x4 mm, driven patches are 2.95 x 2.95 mm, the director 1 elements are 2.81 x 2.81 mm and the single director 2 element is 2.81 x 2.81 mm. The angle,  $\beta$ , between the individual arrays in the “double printed” Yagi antenna array is  $42^\circ$ . The spacing between each element is 140  $\mu\text{m}$ . The feeding structure for this design is printed on the same surface with the elements, due to the fact that sometimes the substrate used in the fabrication is not suitable for processing vias in probe feeding techniques. Additionally, aperture-coupling and proximity coupling feeds often require the use of a multilayer substrate such as low-temperature cofired ceramics (LTCC) or liquid crystal polymer (LCP) which can increase the complexity of the design. By printing the feeding structure on the same surface as the elements, many of these complexities are eliminated. Despite this advantage, this structure can support many feeding structures (aperture-coupling, proximity coupling, coaxial probes, etc...). The feed network consists of an equal power split T-junction where the 50  $\Omega$  line splits into two 100  $\Omega$  lines. Furthermore, the 100  $\Omega$  lines pass through the reflector before feeding the driven elements. Hence, a coaxial-to-waveguide (CPW) mode is excited in each Yagi sub array where the reflector is split into two finite ground planes.

The design in Fig. 7 was simulated using the 3D TLM-based MicroStripes 6.5 by Flomerics, Ltd. The return loss versus frequency is shown in Fig. 8. There are two resonances at 32.2 GHz and 33.4 GHz. The lower resonance occurs from the  $\text{TM}_{10}$  mode of the driven patch, while the higher resonance comes from a parasitic mode that resonates due to the capacitive coupling of energy between the individual arrays. This resonance could be suppressed by increasing the distance between the individual arrays, but significant side-lobe radiation could contaminate the far field radiation. The relative impedance bandwidth is 7%. The presence of the two resonances helps to widen the bandwidth of the antenna. The radiation patterns at 33.1 GHz are shown in Figs. 9 and 10. The co-polarized component of the E-plane elevation pattern exhibits a maximum radiation at approximately  $35^\circ$  with a beamwidth of  $40^\circ$  between  $\theta = 20^\circ$  and  $\theta = 60^\circ$ . The maximum directivity is 12.14 dBi. The cross-polarized component of the

E-plane elevation pattern is below -35 dB. The  $E_0$  component of the azimuth plane radiation pattern at an elevation of  $35^\circ$  is shown to illustrate a reduction of 13 dB at  $\varphi = 180^\circ$  with respect to the direction of maximum radiation along the positive x axis. The azimuthal beamwidth is  $\approx 60^\circ$  ( $-30^\circ$ - $30^\circ$ ). The simulated design exhibits a radiation efficiency of 91%. A lower maximum directivity is exhibited when the angle  $\beta$  between the individual arrays was increased with respect to the current value. In addition, significant sidelobes are present which contaminate the far field radiation. If the angle between the individual arrays is too large, the main beam will shift closer to the broadside direction, thus, destroyed the Yagi effect.

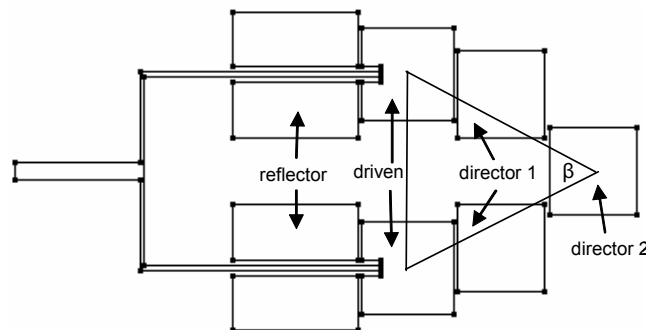


Fig. 7 Microstrip Yagi antenna structure

In order to measure the effectiveness of this design, the dimensions of the antenna were scaled up to operate at 5.2 GHz. The anechoic chamber located in the Technology Square Research Building (TSRB) at Georgia Tech cannot support radiation pattern measurements at mm-wave frequencies. The dimensions of the scaled patch elements are as follows: reflectors are 2.54 x 2.54 cm, driven patches are 1.83 x 1.83 cm, the director 1 elements are 1.73 x 1.73 cm and the single director 2 element is also 1.73 x 1.73 cm. The large feedline at the edge of the substrate has been scaled up accordingly to terminate at 50  $\Omega$ . This scaled antenna design was fabricated at Prototron Circuits Inc. The return loss versus frequency is displayed in Fig. 11. Although the bandwidth of the measured design (9.2%) is slightly greater than that of the simulated design (9.0%), this inconsistency is negligible. A frequency shift at the lower resonance of the measured results can be observed. This shift of 1.5% is reasonable for this type of antenna structure. (Generally, frequency shifts of less than 5% can be attributed to many factors such as measurement inaccuracies, numerical differences in simulation, etc...) The return loss at both resonances in the measured design is higher than that in the simulations. An explanation for this difference has not been determined by the authors of this paper. The co-polarized component of the E-plane radiation patterns for the simulated and measured designs are shown at 5.2 GHz are shown in Fig. 12. The angle of maximum radiation for the measured design is  $36^\circ$ . The efficiency for this design is 90%. The back radiation ( $-90^\circ < \theta < 0^\circ$ ) for this measured design is between 8-10 dB below the main beam. An extension to 6 antennas in a concentric configuration for the transmitter

would enable the full azimuthal (“quasi-omni”) coverage of full-space utilizing 6-sectors of  $60^\circ$  ( $360^\circ/6 = 60^\circ$ ), which equals the beamwidth of each element. A  $40^\circ$  elevation beamwidth would be sufficient for an almost complete, non-intermittent coverage to avoid line-of-sight loss due to human or other objects. A major drawback of this design approach is the backside radiation that exists in the individual structure. An alternative solution would be to place switches in the feedlines and turn one to “ON” state while the others are in “OFF” state to provide  $360^\circ$  radiation,  $60^\circ$  at a time [6,7].

#### IV. IMPROVED MICROSTRIP YAGI ARRAY WITH HIGH F/B RATIO

In order to improve the front-to-back (F/B) ratio of the design considered in Fig. 7, an alternative design has been constructed and is illustrated in Fig. 13. This design, which operates above the 30 GHz band, is smaller than the original design (Fig. 7). Another difference in this design is the use of a single driven element that is excited which produces the radiation. When two driven elements were previously used, the existence of sidelobes in the H-plane radiation pattern was significant. In this improved design, the sidelobes are negligible and multipath from the sides of the antenna can be reduced. The dimensions of this antenna are as follows:  $L_R = 1000 \mu\text{m}$ ,  $W_R = 4016 \mu\text{m}$ ,  $L_D = W_D = 2956 \mu\text{m}$ ,  $L_{D1} = L_{D2} = 2814 \mu\text{m}$ ,  $W_{D1} = W_{D2} = 2014 \mu\text{m}$ ,  $S_1 = 286 \mu\text{m}$ ,  $S_2 = 3686 \mu\text{m}$ , and  $g = 140 \mu\text{m}$ . To feed this structure, microstrip lines were printed on the same layer as the antenna. Instead of using a T-junction feeding network of a  $50 \Omega$  line splitting into two  $100 \Omega$  lines, a quarter-wave transformer line placed between a  $50 \Omega$  line and a high impedance line was used. The operational frequency for this design is 32.7 GHz. The return loss versus frequency is shown in Fig. 8. Again, this design was simulated using MicroStripes 6.5. For this design, the higher resonance is due to the resonant length of the director1 (D1) elements, which is slightly shorter than that of the driven patch. The director2 (D2) elements do not have a major effect on the resonant frequency of this design. The simulated bandwidth for this design is 8.3%. The co-polarized component of the radiation pattern is shown in Fig. 9. The major improvement in this design can be seen in the F/B ratio where the back radiation is defined as radiation between  $-90^\circ < \theta < 0^\circ$ . For this design, a F/B ratio of 16 dB can be observed which is a great improvement in comparison to the F/B ratio (8-10 dB) reported in the original design proposed in Fig. 1. It is believed that the opening in the Fig. 1 design allows for the significantly increased backside radiation, while the Fig. 7 design has an opening in the area of intended radiation, hence, a larger aperture length between the two D2 elements allows for a smaller beamwidth in the pattern and a larger directivity. The maximum directivity achieved for this design is 11.4 dBi, which is slightly smaller than the maximum directivity achieved in Fig. 7. The cross-polarized radiation for this design is below -30 dB in the simulation. This design may be more suitable for providing directional radiation in one direction, then extending to 4-6 in a

concentric configuration to provide full azimuthal (“quasi-omni”) coverage of  $360^\circ$ .

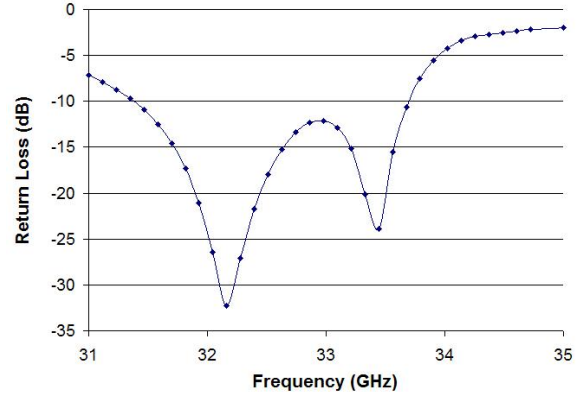


Fig. 8. Simulated return loss versus frequency for 32.5 GHz design

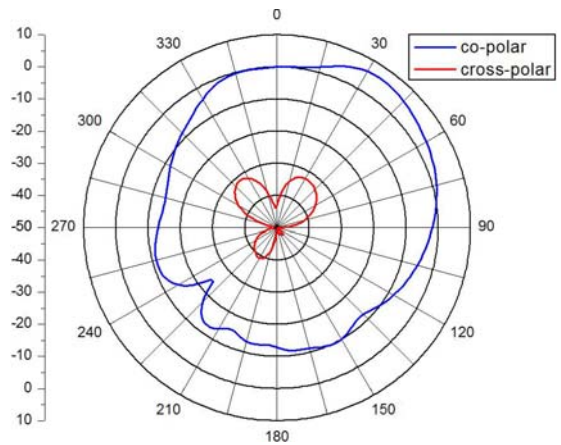


Fig. 9. E-plane co-polar and cross-polar component on elevation plane for 32.5 GHz.

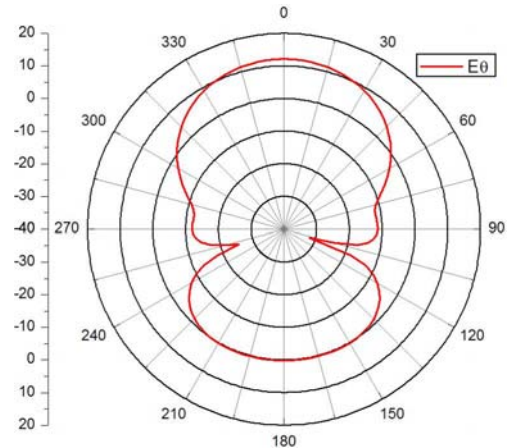


Fig. 10.  $E_0$  component on azimuth plane for 32.5 GHz design.

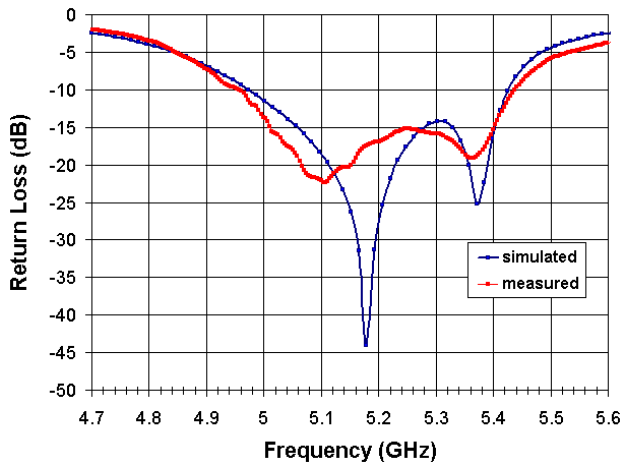


Fig. 11. Return loss versus frequency at 5.2 GHz for Fig. 7 design.

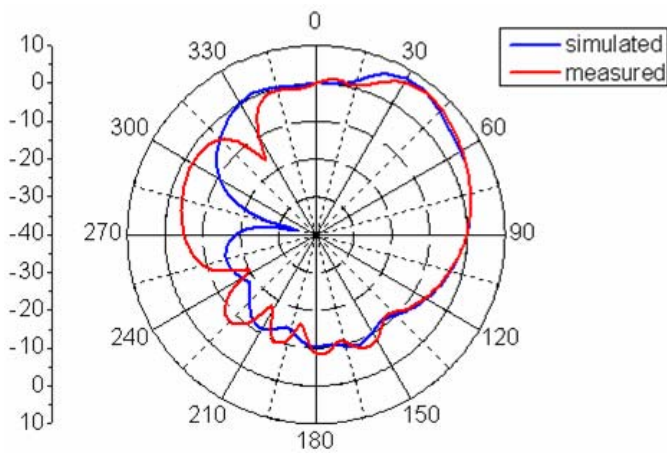


Fig. 12. Co-polarized component on elevation plane at 5.2 GHz for Fig. 7 design.

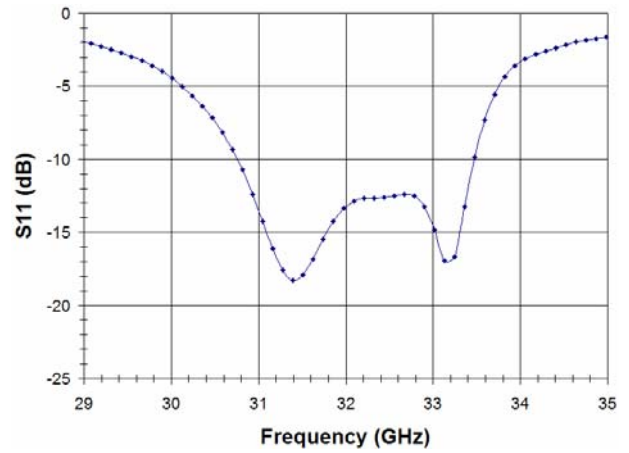


Fig. 14. Return loss versus frequency at 32.7 GHz for Fig. 13 design.

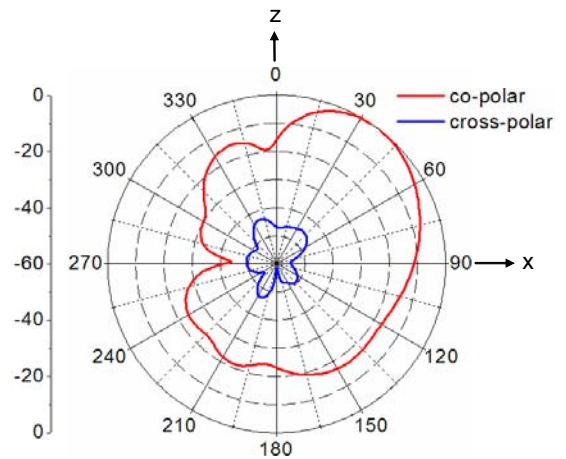


Fig. 14. E-plane co-polar and cross-polar component on elevation plane at 32.7 GHz for Fig. 12 design.

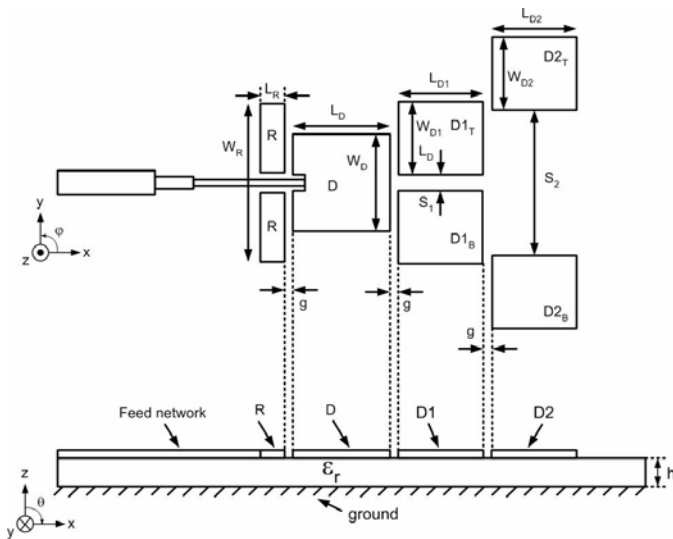


Fig. 13. Antenna structure of improved microstrip Yagi antenna

### Conclusions

Two SoP integration schemes for Yagi-Uda antenna are reported in this paper. One is the W-band vertical Yagi antenna by surface micromachining technology and the other is planar mm-wave Yagi-arrays. Both of them provide low-cost and high performance solution of mm-wave applications.

### References

- [1] R.R.Tummala, M.Swaminathan, M.M.Tentzeris, etc, "The SOP for Miniaturized, Mixed-Signal Computing, Communication and Consumer Systems of the Next Decade", *IEEE Transactions on Advanced Packaging*, Vol.27 No.2, pp.250-267, May 2004.
- [2] Huang, J. *et al*, "Microstrip Yagi array antenna for mobile satellite vehicle application," *IEEE Trans. on Antennas and Propagation*, Vol. 39, Issue 3, 1991, pp. 1024-1030.

- [3] P.P. Vezbicke, "Yagi Antenna Design," *NBS Tech Note 688, National Bureau of Standards*, Washington DC, Dec. 1968
- [4] Yong-Kyu Yoon, Jin-Woo Park, and Mark G. Allen, "RF MEMS Based on Epoxy-Core Conductors," *Digest of Solid-State Sensor, Actuator, and Microsystems Workshop 2002*, , pp.374-375, Hilton Head Island, South Carolina, 2002
- [5] Y.Yoon, B.Pan, J.Papapolymerou, M.M.Tentzeris and M.G.Allen, "A Vertical W-band Surface-Micromachined Yagi-Uda Antenna" , *Procs. of the 2005 IEEE-APS Symposium*, pp.594-597, vol.3A, Washington, DC, July 2005
- [6]. DeJean, G. *et al*, "Liquid crystal polymer (LCP): a new organic material for the development of multilayer dual-frequency-dual-polarization flexible antenna arrays," *IEEE-AWPL*, Vol. 4, 2005, pp. 22-26.
- [7] Gray, D. *et al*, "Electronically steerable Yagi-Uda micro patch antenna array," *IEEE Trans. on Antennas and Propagation*, Vol. 46, Issue 5, 1998, pp. 605-608.